

Computer Simulations of Surfactant Mixtures at the Liquid/Liquid Interface

Hector Domínguez[†]

Instituto de Química, UNAM, Universidad Nacional Autónoma de México, México, D.F. 04510

Received: December 4, 2001; In Final Form: March 18, 2002

We performed molecular dynamics simulations on monolayers of surfactant mixtures at the water/carbon tetrachloride interface. The mixture was composed of sodium dodecyl sulfate (SDS) anionic surfactants and molecules that were chosen to be identical to SDS except that the charges were different in order to make them nonionic. Simulations were conducted for different concentrations of the monolayer mixture; i.e., at a fixed surface area we kept the number of SDS molecules constant while the number of the nonionic molecules was increased. Simulations of different SDS/nonionic mixtures show that the location of the surfactants in the interface is determined by the interaction and the charge distribution of the molecules. We also observe that the structure of the two different surfactants in the monolayer is different and is affected by the concentration of the mixture. For a particular SDS/nonionic mixture, the results indicate that the tails of the SDS molecules are less ordered than the tails of the nonionic molecules. We also show that the length of the SDS chains is shorter than that of the nonionic chains in the same mixture. To investigate the behavior of the SDS molecules in one component monolayer and in the mixture, we also performed simulations of monolayers composed of just SDS molecules at the same surface coverage of the mixtures. The results show that the SDS tails are slightly more disordered in the mixture than in the single monolayer. Finally, the electrostatic potential difference across the interface was also investigated in the mixtures and we find that it increases or decreases depending on the interactions (charge distribution) of the SDS and nonionic molecules in the mixture.

1. Introduction

Studies of surfactant molecules at liquid/vapor and liquid/liquid interfaces have been the subject of investigations for a long time, not only for their scientific interest but also for their applicability in the industry. The study of structural and dynamical properties of these systems has been conducted using different experimental techniques including fluorescence, resonance Raman scattering, neutron reflection, second harmonic generation, vibrational sum-frequency spectroscopy, and time-resolved quasi-elastic laser.^{1–10} Most of these experiments were conducted in systems where there was only one kind of surfactant molecule. However, most commercial products consist of a mixture of surfactants that have richer properties than individual ones. The study of surfactant mixtures has also been investigated using several experimental techniques such as calorimetry, X-ray, neutron scattering, and surface tension measurements among others.^{11–23} There are also theoretical efforts in this field.^{24,25} These studies have been performed for mixtures of anionic–anionic, cationic–cationic, nonionic–nonionic surfactants, and combinations of those molecules. Of particular interest is the study of anionic–nonionic mixtures since nonionic surfactants are generally used together with anionic surfactants as active ingredients in products such as shampoo, hand dish washing liquids, and washing powders.

In the last years, special attention has been paid to the study of the structure and composition of surfactant mixtures at interfaces, e.g., the position of the surfactants at the interface (the location of the molecules along the solvent), the extension of the chains, the thickness of the monolayer mixture, etc.^{16,19,21–23,26} For instance, Lu et al.²³ observed by neutron reflection experiments of dodecanol and sodium dodecyl sulfate

at the air/water interface, differences in the position of the molecules along the interface. The SDS seemed to penetrate more into the solvent than the dodecanol. They also found that the dodecanol molecule is slightly thicker than the SDS and it is less tilted than the SDS in the monolayer. On the other hand, Penfold et al.¹⁹ conducted experiments of cationic–nonionic (C₁₆TAB/C₁₂E₆) surfactants and they found an increasing change in position of the nonionic molecules at the interface relative to the solvent with increasing solubility of the nonionic molecules.

The position of the different surfactants in the interface might be attributed to the different polar group of the molecules; i.e., the interaction between surfactant molecules is influenced by the nature of the headgroup. Surface tension experiments have shown that mixtures with similar hydrophobic tail lengths but with different headgroups may show different properties that can affect the structure of the monolayer at the interface. For instance Goloub et al. observed that nonionic mixtures present a more ideal behavior compared to the anionic–nonionic mixtures.¹¹ On the other hand, other authors have been more interested in the study of the adsorption of surfactant mixtures at different interfaces and the lowering of the interfacial tension by the presence of surfactant mixtures.^{27–29}

Due to the substantial increase in computational power over the last years, computer simulations became an important tool for the study of such complex interfacial systems.^{30–36} These kinds of studies allow us to extract more information about dynamical and structural properties of interfacial problems from a molecular level, which are not easy to get from real experiments. One of the conveniences of using computer simulations is the possibility of studying, with an appropriate model, either general or particular properties of a system. Moreover, variations of the model could help us better to

[†] E-mail: hectordc@servidor.unam.mx.

TABLE 1: Atomic Charge in Each Site of the Head Group of the SDS, SDSN, and SDSE Molecules

	<i>q</i> (charge)		
	SDS	SDSN	SDSE
S	1.284	1.284	−1.284
O (SO ₃)	−0.654	−0.654	0.654
O ester	−0.459	−0.459	0.459
CH ₂ attached to O	0.137	1.137	−1.137

understand situations that are not possible in real experiments. The present investigation of surfactant monolayers was carried out by molecular dynamics computer simulations.

In this paper, we investigate the behavior of anionic–nonionic surfactant mixtures at the water/carbon tetrachloride interface. We analyze how the charge distribution of the molecule heads might affect the monolayer configuration in the interface. We also study the orientation and order of the molecule chains at the interface. We used one of the most common surfactants, sodium dodecyl sulfate (SDS), as a prototypical anionic surfactant. The nonionic surfactant was created by a model that is identical to the SDS except in the distribution of the atomic charges. In this way we were able to have different nonionic molecules by changing the charge distribution of the headgroup.

Several simulations were conducted at different surface coverages, i.e., different areas per headgroup. In all cases the number of SDS molecules in the monolayer was kept constant, while the concentration of the nonionic molecules was increased. To compare how the SDS molecules were affected in the mixture by the presence of one particular nonionic molecule, we also performed simulations of monolayers composed of just SDS molecules at the same interface and at the same surface coverage of the monolayer mixtures.

2. Computational Method and Model

For the present study we performed simulations of two kind of monolayers: one composed of a mixture of anionic and nonionic molecules and the second one composed of just anionic molecules. For the anionic molecules we used a SDS molecule model of a hydrocarbon chain of 12 united carbon atoms attached to a headgroup SO₄. The headgroup atoms were explicitly modeled. The simulation parameters for the SDS were the same used in previous works.^{32,36} Following the same spirit for constructing a new molecule by keeping the structure of a known one,³³ we constructed the nonionic molecule with the same SDS model except that we changed the charge distribution. Mainly, we removed the sodium anion and we modified the charge distribution in the headgroup (see Table 1). All the other simulation parameters were the same as for the SDS molecule. We call the nonionic molecule SDSN. The same SDS molecular structure for the nonionic molecules allowed us to control the same surface coverage, chain length, and headgroup geometry, while focusing only on the effects of the anionic–nonionic interactions.

For reasons that will be discussed later in the Results, we also constructed another nonionic molecule. The new molecule was different from the SDSN molecule in the head charge distribution (see Table 1). Mainly the sign of all the charges were reversed; i.e., we replaced positive charges by negatives and vice versa. The molecule tails were the same as in the SDSN and SDS molecules. We call the new nonionic molecule SDSE. Although the new molecules do not have the structure of a real known nonionic surfactant, they have the components of a nonionic molecule. However, due to the “artificial” nonionic molecule models the comparisons with real experiments are not

straightforward. Nevertheless, we believe that the choice of these two nonionic molecules will allow us to establish how the polar headgroup of the surfactants affect the structure of the monolayer and perform, when and where possible, some comparison with experiments. We consider they will show us new insights of how the anionic–nonionic molecules behave under different interactions with their headgroups and they will show us how the molecules are oriented and ordered at the interface.

For water molecules we used the SPC model and for carbon tetrachloride, CCl₄, we used the same rigid molecule as in our previous work.³⁶ All simulations were carried out in the NVT ensemble with a time step of 0.002 ps using the DL-POLY package.³⁷ Bond lengths were constrained using the SHAKE algorithm with a tolerance of 10^{−4}. The temperature was controlled using the Hoover–Nose thermostat with relaxation time of 0.2 ps.³⁸ All simulations were performed at *T* = 300 K. For the long-range electrostatic potential we used the Particle Mesh Ewald method with precision of 10^{−4} and the van der Waals interactions were cut off at 10 Å.

The initial configuration was prepared similarly as in ref 36. First, we constructed the monolayer of just SDS molecules. Then, from that monolayer we prepared the monolayer mixture. A monolayer initially composed of 40 SDS molecules in all-trans configuration was placed in a square box with *x* and *y* dimensions of 46.09 Å. This configuration corresponds to an area per headgroup of 53.1 Å²/molecule, which is slightly lower than the saturation area of 59 Å²/molecule for a monolayer at the water/CCl₄ interface.⁵ The *z*-dimension of the box was set to 150 Å. This length was long enough to accommodate two liquid slabs and to prevent the formation of a second water/CCl₄ interface. Instead, two vapor/liquid interfaces at the opposite ends of the box (on the *z* < 0 side the vapor/water interface and on the *z* > 0 side the liquid CCl₄/vapor interface) were present in the box.

With the molecules of the headgroup initially pinned, we performed a short MD simulation at *T* = 300 K. Then, the temperature was increased to 400 K in order to randomize the tails. Subsequently, the temperature was decreased in short runs until we reached *T* = 300 K. At this point we added 1185 water molecules surrounding the headgroups and a layer of 415 CCl₄ molecules was placed in the region of the tails. Water was placed at *z* < 0 and CCl₄ at *z* > 0. The system was then equilibrated for 100 ps. Finally, 40 sodium anions were randomly inserted in the interfacial region. This final configuration was then equilibrated for 300 ps. The initial configuration of the SDS monolayers for different areas per headgroup was constructed from the one already described. From the initial monolayer of 40 SDS molecules at the water/CCl₄ interface and with the same square area, we added groups of 4 or 8 SDS molecules in order to have 2 more different monolayers with areas per headgroup of 48.3 and 44.3 Å²/molecule, respectively. Then, with their headgroups pinned, we ran each system for 25 ps. The corresponding number of sodium anions atoms were also placed in the interfacial region for each case. Finally, each system was equilibrated for an extra 300 ps. These monolayers will be called single monolayers to differentiate them from those composed of a mixture of surfactants. The monolayers with 40, 44, and 48 SDS molecules will be named M40, M44, and M48, respectively.

Preparation of the SDS/SDSN monolayers was performed as follows. Before the final equilibration of the single monolayers, for example in M40, we replaced 2 SDS molecules by 2 SDSN molecules removing also 2 sodium anions. In the same way, from the monolayer of 44 SDS molecules we replaced 6 SDS

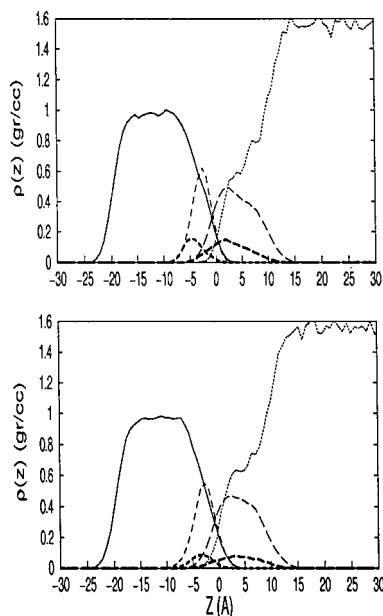


Figure 1. Density profile for the SDS/SDSN monolayer at the $\text{CCl}_4/\text{water}$ interface. The top picture corresponds to the monolayer of 38 SDS molecules with 10 SDSN molecules. The bottom picture represents the monolayer of 38 SDS molecules with 6 SDSN molecules. Water is depicted by the solid line, CCl_4 by the dotted line, the SDS headgroups by the short light dashed line, and the SDS tails by the long light dashed line. The SDSN headgroups are given by the short dark dashed line, and SDSN tails, by the long dark dashed line.

molecules by 6 SDSN molecules, removing also 6 sodium anions. Subsequently, the same procedure was carried out for the last of the monolayer M48, where we replaced 10 SDS by 10 SDSN molecules. In all cases the number of SDS molecules was fixed to 38. In this way we prepared 3 different monolayer mixtures. Once these monolayers were prepared, they were simulated for 25 ps with the headgroups pinned. Finally, with the headgroups free, each system was equilibrated for an extra 300 ps. These monolayer mixtures will be called MN2, MN6, and MN10 for the case when there are 2, 6, and 10 SDSN with 38 SDS molecules in the monolayer. The SDS/SDSE monolayers were prepared exactly in the same way as above, just replacing SDSN for SDSE molecules. However, we just simulated monolayers with 6 and 10 SDSE molecules. These monolayer mixtures will be called ME6 and ME10. All the simulations were performed up to 1.25 ns run and we collected data from the last 500 ps for analysis. Configurational energy was monitored as a function of time as a parameter to determine when the system reached equilibrium.

3. Results

In this section we present the calculations performed in the monolayer mixture and in the one-component monolayer. Analysis of the structure, orientation, and order of the tails of the two different surfactants are discussed.

3.1. Density Profile, Headgroup, and Hydrocarbon Chain Distribution. The first analysis was performed for the density profiles. In Figure 1 we show the profiles of two characteristic monolayer mixtures, MN6 (bottom) and MN10 (top). The z -dependent density profiles for the liquids, headgroups, and hydrocarbon tails of each surfactant molecule, SDS and SDSN, are plotted separately. In this way it is possible to make a distinction of the distribution of the SDS and the SDSN molecules along the interface. The SDS headgroup density profile includes the SO_4^- group and the Na^+ counterion. Since

TABLE 2: Average Mean Position (Z_0) and Width (σ^2) of the Density Profiles of the Head Groups (HG) and the Tails of the Monolayer Mixtures^a

no. of nonionic molecules	HG		tail		molecule
	Z_0 (Å)	σ^2 (Å)	Z_0 (Å)	σ^2 (Å)	
2	-3.0	32.3	3.2	125.7	SDS
MN2	-4.8	40.3	3.0	153.4	SDSN
6	-2.7	34.6	3.8	138.0	SDS
MN6	-3.3	32.9	3.8	137.3	SDSN
10	-2.7	27.4	3.9	139.0	SDS
MN10	-4.4	28.7	2.5	115.6	SDSN
6	-3.1	29.2	3.2	123.3	SDS
ME6	-2.1	25.0	3.7	127.8	SDSE
10	-2.7	41.5	3.6	151.4	SDS
ME10	-1.2	23.4	4.3	126.3	SDSE

^a Top data are for the SDS and SDSN molecules in the MN2, MN6, and MN10 monolayers. Bottom data are for the SDS and SDSE molecules in the ME6 and ME10 monolayers. The number of SDS molecules is fixed to 38. The values correspond to the molecules indicated in the rightmost column.

there are more SDS than SDSN molecules, the profiles of the headgroups and the tails of SDS are obviously higher than the SDSN in both pictures. For the mixture M2, there are even less SDSN molecules and their profiles are too small compared to the SDS ones. However, what is interesting to observe is the average position, calculated by fitting a Gaussian, of the profiles of the headgroups and the tails (Table 2). The Gaussian distribution used was the following:

$$\rho = \rho_0 \exp\left(\frac{-4(Z - Z_0)^2}{\sigma^2}\right) \quad (1)$$

The headgroup of the SDS molecules, for MN6 and MN10 (see Figure 1), is slightly shifted toward the oil with respect to the headgroup of the SDSN molecules; see Table 2. The distance difference between the profiles in the case of the headgroups is 0.6 and 1.7 Å for MN6 and MN10, respectively. In the case of the tails, the distance difference is less than 1.0 Å (≈ 1.4 Å for MN10). A similar trend was observed for the other density profiles of the monolayer mixture at different SDSN concentration, MN2. In neutron reflection experiments at 300 K of monolayer mixtures of SDS/dodecanol at the water/air interface it is observed that the SDS volume fraction profile is displaced toward the water, for about 3.5 Å from the dodecanol profile.^{19,23} When we analyzed only the distribution of sulfur atoms in the headgroups of the SDS and SDSN molecules (Figure 2), we found the same trend as on the headgroups. In Figure 2, the distribution of the sulfur atom “SN” of the SDSN molecules (top) and the sulfur atom “S” of the SDS molecules (bottom) of all monolayers, MN2, MN6, and MN10, is plotted. For all of them, we observe that the “SN” profiles are slightly shifted to the left of the “S” profiles in the same monolayer.

Due to the discrepancy of the results observed with the experiments, we conducted other simulations with another monolayer mixture, i.e., the SDS/SDSE monolayer discussed in the previous section. The new simulations were just performed for systems with higher nonionic molecule concentrations; i.e., we ran monolayers with 6 and 10 SDSE and 38 SDS molecules (ME6 and ME10). In Figure 3 we show the density profiles for the SDS/SDSE mixture. As can be observed, the SDSE headgroup density profile in this case is shifted to the right of the SDS; i.e., the SDS headgroup is located toward the water. The same trend occurs for ME6 and ME10. The distance

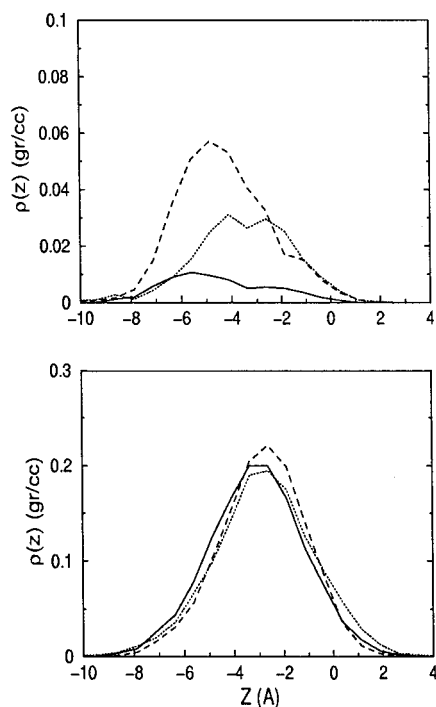


Figure 2. Density profile of the sulfur atoms of the SDS/SDSN monolayer mixture. The top picture shows the sulfur “SN” atom of the SDSN headgroup, and the bottom picture is for the sulfur “S” atom of the SDS headgroup. The solid line represents the monolayer MN2, dotted line the MN6, and short dashed line the MN10.

difference between the profiles of the headgroups is ≈ 1.0 and 1.5 Å for ME6 and ME10, respectively. The average position of the density profiles are given in Table 2. These new results are in agreement with the experiments mentioned above.^{19,23} In Figure 4 we also show the profiles of the sulfur atom (“SE”) of the SDSE molecule and the sulfur atom (“S”) of the SDS. They present the same trend as in Figure 3, the “SE” atoms are slightly shifted to the right of the “S” atoms. To understand the behavior of the position of the surfactants in the interface in the two monolayers, we did a rough and simple analysis of the charges in the SDSN and SDSE molecule headgroups. If we group the charges of the SO_4^- in a single site (centered in the sulfur atom “S”) and the CH_2 charge (the first carbon) in another site, we could assign an average dipole orientation to the molecule headgroups. For MN6 and MN10 the dipole of the SDSN headgroup is inclined 45° and 38° , with respect to the normal of the interface, respectively, and it points to the negative z -axis (water phase). For the ME6 and ME10 monolayers the dipole of the SDSE headgroup makes an angle of 77° and 80° , respectively. The dipoles are more inclined than those for the SDSN molecules. Moreover, they are directed toward the positive z -axis. We observe that the dipole orientation of the SDSE molecule headgroup is in opposite z -direction of the SDSN molecule. On the other hand, the water dipole in the interface region is in the negative z -axis with an angle of 71° – 80° (depending of the monolayer). In previous simulations of SDS monolayers at the water/ CCl_4 interface, they found that the water dipole makes an angle of 75° .³³

In the case of the “MN” monolayers, the negative SO_4^- group of the SDS molecule is stable with the water molecules at the interface. However, since the water and SDSN dipole moment are in the same z -direction, the SDSN dipole (the headgroup) should go deeper into the aqueous media to be more electrically stable. Then, the SDSN molecules are shifted to the water respect to the SDS molecules in the z -axis.

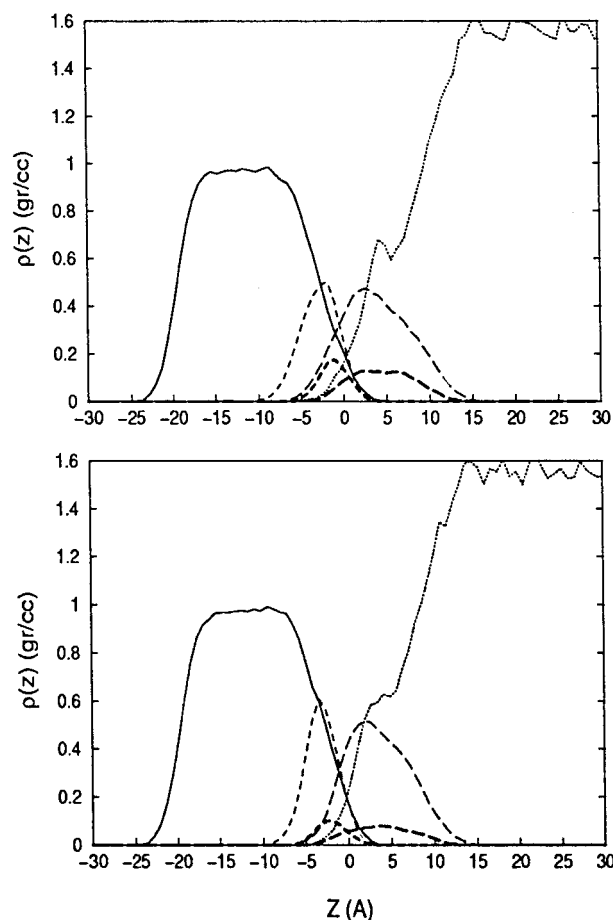


Figure 3. Density profile for the SDS/SDSE monolayer at the CCl_4 /water interface. The top picture corresponds to the monolayer of 38 SDS molecules with 10 SDSE molecules. The bottom picture represents the monolayer of 38 SDS molecules with 6 SDSE molecules. Water is depicted by the solid line, CCl_4 by the dotted line, the SDS headgroups by the short light dashed line, and the SDS tails by the long light dashed line. The SDSE headgroups are given by the short dark dashed line, and SDSE tails, by the long dark dashed line.

In the case of the “ME” monolayers, a different feature occurs. The water dipole and the dipole of the SDSE headgroup point in opposite direction, so the SDSE headgroup can be stable at the interface. However, the negative SO_4^- group of the SDS is more electrically stable deeper into the water, shifting from the SDSE molecule.

The orientation of the headgroup of each surfactant in the mixture is calculated from the total length measured from the most opposite oxygen atoms (δ_{hg}) and the projection of the headgroup along the normal to the interface (δ_{zhg}), $\delta_{\text{zhg}}/\delta_{\text{hg}}$. In the SDS/SDSN mixture, the angle that the SDS headgroup makes with the normal is slightly higher than that of the SDSN, indicating that the headgroup of the SDS somehow is more bent toward the interface plane. For MN2 the angle of the headgroup with the normal to the interface is 55° and 43° for the SDS and SDSN molecules, respectively. For MN6, the angle is 54° and 50° for the SDS and SDSN molecules, respectively. For MN10, the angle is 51° and 50° for the SDS and SDSN molecules, respectively. These results are in agreement with our previous observation that the SDS headgroup profile is shifted to the right of the SDSN headgroup profile. In the SDS/SDSE mixture we observe that the headgroup of the SDSE is lightly more bent than that of the SDS. For ME6, the angle of the headgroup with the normal to the interface is 51° and 54° for the SDS and SDSE molecules, respectively. For ME10, the angle is 51° and 56° for the SDS and SDSE molecules, respectively.

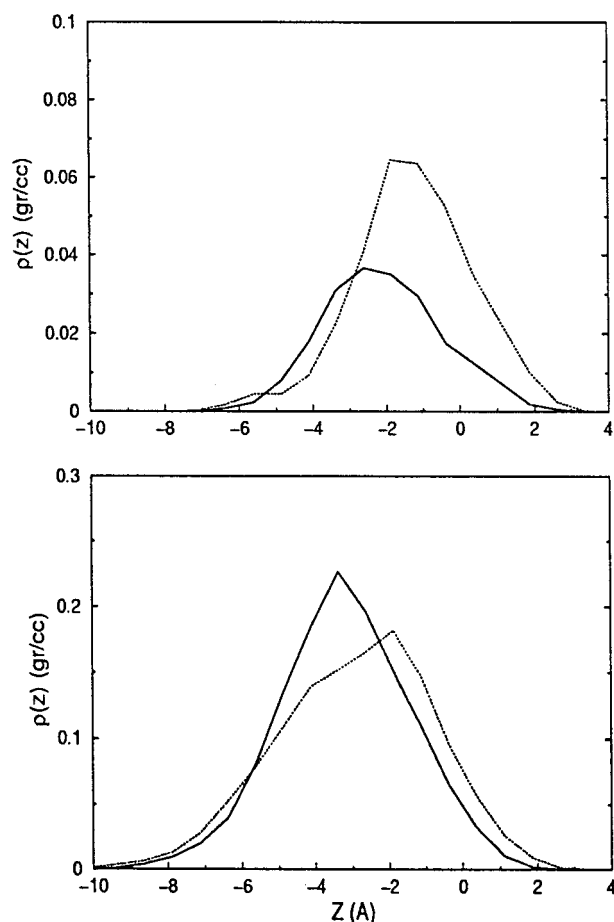


Figure 4. Density profile of the sulfur atoms of the SDS/SDSE monolayer mixture. The top picture shows the sulfur “SE” atom of the SDSE headgroup, and the bottom picture is for the sulfur “S” atom of the SDS headgroup. The solid line represents the monolayer ME6, and the dotted line, the ME10.

3.2. Electrical Potential. A real difference between the two surfactant molecules, which form the monolayer mixture, is their charge. So, we measured a property that is connected directly with the distribution of charges in the system. For this case we analyzed the electric potential of the different monolayer mixtures. In the computer simulations, the electrical potential was calculated using the formula

$$\Delta\phi = \phi(z_2) - \phi(z_1) = - \int_{z_1}^{z_2} dz' E_z(z') \quad (2)$$

where the electric field is given by

$$E_z(z) = \frac{1}{\epsilon_0} \int_z^{z_1} dz' \rho_q(z') \quad (3)$$

Here $\rho_q(z)$ is the charge density. The reference potential $\phi(z_1) = 0.0$ V was chosen in the vacuum region ($z < 0$) far from the interface. In the calculation of the potential we included in the forces the surface term as discussed in early works.^{36,39}

In Figure 5, the charge density profile, the electric field and the potential difference across the interface are plotted for the monolayers MN6 and MN10. We observed that the charge density profile does not show much difference between the monolayers in comparison with the electrostatic field where a more significant difference can be appreciated. However, a higher difference is observed in the surface potential. Measuring the potential difference across the interface, we find that this value is higher in MN10 than in MN6 and MN2. Furthermore,

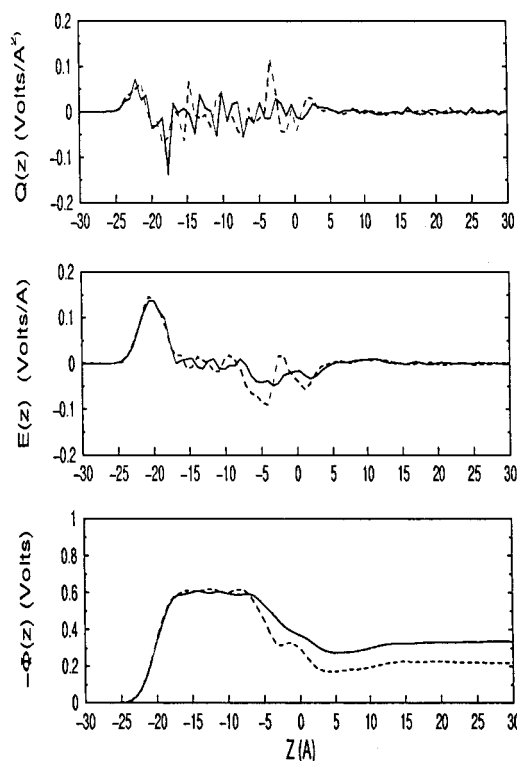


Figure 5. Charge density profile for the SDS/SDSN monolayer mixture at the CCl₄/water interface (top panel). The electric field is depicted in the middle, and the potential profile, in the bottom panel. The solid line is for MN6, and the dashed line, for MN10.

we found that the potential difference gets higher as we increase the concentration of the SDSN molecules in the monolayer mixture. For the monolayers MN2, MN6, and MN10 we have potential differences of 253, 265, and 385 mV, respectively. A significant jump, of about 45% in the potential difference, is presented from monolayer MN6 to MN10.

We also calculated the charge density, the electrical field, and the potential in monolayers ME6 and ME10 (Figure 6). We observed a variations in the electrical properties for the different mixtures. However, the electrical potential showed a significant difference in comparison with the MN monolayers. On the contrary of the MN, for the ME monolayers the potential difference decreases as the SDSE (nonionic) molecules increases. For the ME6 and MN10 the potential difference is 320 and 226 mV, respectively.

3.3. Surface Tension. The surface tensions were calculated by the quantity Γ ,

$$\Gamma = L_z (\langle P_n \rangle - \langle P_t \rangle) \quad (4)$$

where $\langle P_n \rangle$ is the normal pressure, $\langle P_t \rangle$ is the average tangential pressure, and L_z is the length of the box in z -direction. When the simulation box contains several interfaces, the value of Γ is equal to the surface tension γ of each interface

$$\Gamma = \sum \gamma_i \quad (5)$$

For instance, in the vapor/water/CCl₄/vapor system

$$\Gamma = \gamma_{v/w} + \gamma_{w/o} + \gamma_{o/v} \quad (6)$$

where $\gamma_{v/w}$ is the surface tension for the vapor/water interface, $\gamma_{w/o}$ is the surface tension for the water/organic liquid interface and $\gamma_{o/v}$ is the surface tension for the organic liquid/vapor interface. In the presence of surfactant molecules at the water/

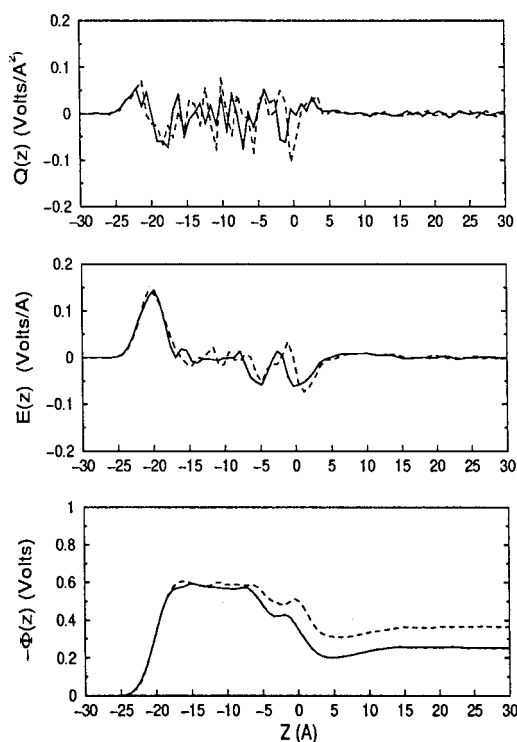


Figure 6. Charge density profile for the SDS/SDSE monolayer mixture at the CCl_4 /water interface (top panel). The electric field is depicted in the middle, and the potential profile, in the bottom panel. The solid line is for ME6, and the dashed line, for ME10.

CCl_4 interface the surface tension of the interface water/organic liquid will be changed, $\tilde{\gamma}_{w/o}$. To calculate the change, we need to find the values of the surface tensions for the vapor/water and CCl_4 /vapor interfaces. These values were calculated in our previous work,³⁶ where we found $\gamma_{v/w} = 68.8 \pm 4$ mN/m and $\gamma_{o/v} = 21.4 \pm 3$ mN/m for the water/air and CCl_4 /air interfaces, respectively (the experimental values are 72 and 26.9 mN/m^{40,41}).

The surface tension of the single monolayer at the vapor/water/SDS/ CCl_4 /vapor is 106.4 ± 4 , 97.1 ± 6 , and 99.4 ± 5 for M40, M44, and M48, respectively. The value of the surface tension of M48 is in good agreement with the one calculated in a previous work (100.7 ± 6) using an area per headgroup of 45 \AA^2 .³⁶ In the case of the monolayer mixtures, the surface tension vapor/water/SDS–SDSN/ CCl_4 /vapor was 108.0 ± 6 , 107.7 ± 5 , and 107.1 ± 6 for MN2, MN6, and MN10, respectively. Therefore, from eq 6 we obtained that in the presence of the monolayer mixture $\tilde{\gamma}_{w/o}$ is 17.8 ± 13 , 17.5 ± 12 , and 16.9 ± 13 for MN2, MN6, and MN10, respectively. In the case of the monolayer composed of just SDS molecules $\tilde{\gamma}_{w/o}$ is 16.2 ± 11 , 6.9 ± 13 , and 9.2 ± 12 for M40, M44, and M48, respectively. Due to the analysis of errors, the values of the surface tension are close to each other within the error bars. Nevertheless, the surface tensions of the mixtures are slightly higher than those in the single monolayers for the same surface coverage.

Results of the surface tension for the ME6 and ME10 monolayers were also analyzed. For the surface tension vapor/water/SDS–SDSE/ CCl_4 /vapor, we found the values of 103.1 ± 4 and 107.8 ± 5 for the ME6 and ME10, respectively. Therefore, $\tilde{\gamma}_{w/o}$ is 12.9 ± 11 and 17.6 ± 12 for the ME6 and ME10, respectively. In this case it seems that the surface tension slightly increases with the nonionic molecule compared with the MN monolayers where the surface tension slightly decreases with the nonionic molecules. However, the differences in the

TABLE 3: Angle, of the Tails of the Surfactant Molecules in the Mixture, with Respect to the Normal of the Interface and Total (δ) and projection (δ_z) lengths of the SDS and SDSN tails of the monolayer mixtures, MN2, MN6, AND MN10^a

no. of SDSN molecules	tail			molecules
	δ_z (Å)	δ (Å)	angle (deg)	
2	8.3	11.5	44	SDS
MN2	10.4	11.9	29	SDSN
6	8.6	11.5	42	SDS
MN6	10.1	12.0	33	SDSN
10	8.9	11.4	39	SDS
MM10	8.7	11.4	40	SDSN

^a The number of SDS molecules is fixed to 38.

surface tensions are too small and due to the error bars it is not clearly indicated if they present a real change in each value.

3.4. Hydrocarbon Tails, Length, and Tilt Angle. For the last subsections, the analysis of orientation and order of the chains are presented in more detail for the SDS/SDSN monolayer mixtures. For the SDS/SDSE mixture similar trends were observed. Total length of the tails, δ_t , was measured as the distance from the first carbon to the last carbon in the chain. The projection of the chains along the normal to the interface, which some people call the thickness δ_z of the monolayer, was also calculated. To study the difference between the SDS and the SDSN molecules in the mixture, we calculated separately the average length of the tails for each molecule in the monolayer. From the data in Table 3, we see that the length and thickness of the SDSN tails are almost always larger than those of the SDS tails. Depending on the surface coverage of each monolayer mixture, the difference in the total length of the tails of SDS and SDSN can be up to 0.5 \AA (MN6), whereas the difference in the thickness can be up to 2.1 \AA (MN2). A rough estimate of the chain tilt can be obtained from the ratio between δ_z and δ_t , i.e., $\cos \theta = \delta_z/\delta_t$. The average tilt angle (Table 3) indicates that the tails of the SDS molecules seem to be more bent than the tails of SDSN. The highest difference in the tilt angle between the SDS and the SDSN tails is $\approx 15^\circ$ for the MN2 monolayer. From Table 3 we also observe that there is a tendency of decreasing the tilt angle of the SDS tails whereas the tilt angle of the SDSN chains increases as the concentration of SDSN increases. The experiments of neutron reflection of SDS–dodecanol at the water/air interface, conducted by Lu et al. showed that the thickness of the dodecanol is larger than the thickness of the anionic surfactant.²³ From the same experiments, they also observed that the tilt angle of the SDS chain is higher than that of the dodecanol.

To obtain more information about the inclination of the tails, we calculated the average angle between the C_1 – C_n vector (C_1 first carbon and C_n the n -carbon in the tail, $n = 2, 3, \dots, 12$) and the normal to the interface. Figure 7 shows the results for the SDS (bottom picture) and the SDSN tails (top picture) of all the monolayer mixtures studied here. From Figure 7 we observe that the angles of the carbons, for almost all the tails, reach nearly a plateau at the end, indicating that they have the same inclination. The $\cos \theta$ of the carbons of the SDSN tails decays as the concentration of SDSN molecules increases. An interesting feature from Figure 7 is the angle of the second carbon in the tails for both the SDS and SDSN molecules. That angle is always higher for the SDS than for the SDSN, indicating that the tails of the nonionic molecules are more straight at the beginning of the chain than the tails of the anionic molecules.

To study how the tails of the SDS molecules are affected by the inclusion of the SDSN, we also calculated the total length

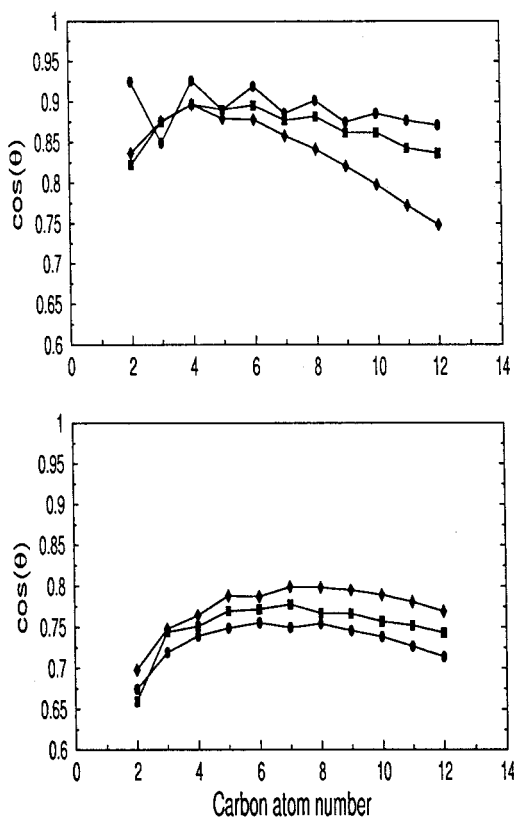


Figure 7. Cosine of the angle between the C_1-C_n ($n = 2, 3, \dots, 12$) vector and the vector normal to the interface of the surfactant molecules in the SDS/SDSN monolayer mixture. The top picture shows the $\cos \theta$ of the SDSN tails, and the bottom picture, the $\cos \theta$ of the SDS tails in the same monolayer for all the mixtures. Circles are for MN2, squares are for MN6, and diamonds represent MN10.

TABLE 4: Angle, of Tails of the SDS One Component Monolayer, with Respect to the Normal of the Interface and Total (δ) and Projection (δ_z) Lengths of the Single Monolayers, M40, M44, and M48

no. of SDS molecules	tail		
	δ_z (Å)	δ (Å)	angle (deg)
40	7.8	11.4	47
44	9.3	11.5	36
48	9.5	11.7	36

(thickness) and tilt angle of the chains in the single monolayers (M40–M48) at the same surface coverage of the monolayer mixtures. These data are given in Table 4. From these numbers we observe that the total length and the thickness of the SDS tails in single monolayers (M44 and M48) are slightly larger than those (MN6 and MN10) in the mixture. For M40, the reverse trend occurs. The tilt angles indicate that the SDS tails in the mixture are slightly more bent than the SDS tails in the single monolayer. Results for M48 are in good agreement with our previous simulations of a SDS monolayer at the water/ CCl_4 interface with an area per headgroup of $45 \text{ Å}^2/\text{molecule}$.³⁶ In Figure 8, the average angle between the C_1-C_n vector and the normal to the interface is shown. From this figure we see that the tails get more straight as the number of SDS molecules increase for the same interfacial area. Tails of M44 and M48 have similar inclination.

3.5. Order Parameters and Number of Gauche Defects.

The ordering of the tails in phospholipid membranes is usually characterized by the so-called deuterium order parameter, S_{CD} , which shows the average inclination of the C–D bond with respect to the bilayer normal. For these measurements, the

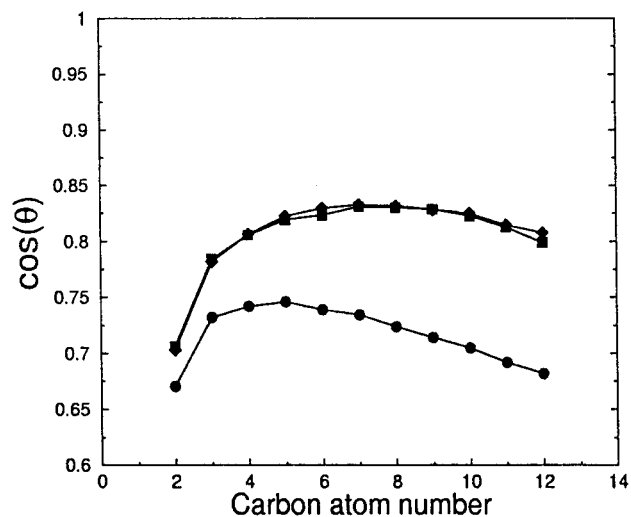


Figure 8. Cosine of the angle between the C_1-C_n ($n = 2, 3, \dots, 12$) vector and the vector normal to the interface for the SDS one component monolayer. Circles are for M40, squares are for M44, and diamonds represent M48.

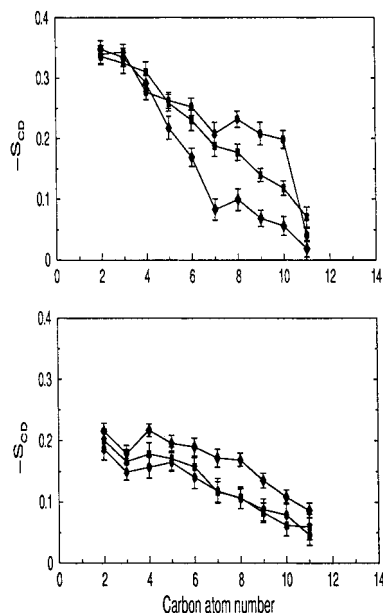


Figure 9. S_{CD} order parameter as a function of the carbon position of the surfactant molecules in the SDS/SDSN monolayer mixture. The top picture shows the order in the carbons of the SDSN tails, and the bottom picture is the order of the carbons of the SDS tails in the same monolayer for all the mixtures. Circles are for MN2, squares are for MN6, and diamonds represent MN10.

hydrogens of the chains are selectively replaced by deuteriums and the NMR technique is used. In computer simulations that use united CH_n atoms, the S_{CD} order parameter is calculated using the following formula:⁴²

$$S_{\text{CD}} = (2/3)S_{\text{xx}} + (1/3)S_{\text{yy}} \quad (7)$$

$$S_{ij} = (1/2)\langle 3 \cos \theta_i \cos \theta_j - \delta_{ij} \rangle \quad (8)$$

$i, j = x, y, z$ and θ_i is the angle between the i th molecular axis and the normal to the interface (see the details in ref 42).

The order parameter of the carbons for the SDS and SDSN molecules in the same monolayer is calculated separately. Figure 9 shows the results. The S_{CD} order parameter for carbons in the SDS molecules gets higher as the SDSN concentration increases

TABLE 5: Total Average Order Parameter, $\langle |S_{CD}| \rangle$, and Average Number of Gauche Defects of the SDS and SDSN Tails in the Monolayer Mixtures, MN2, MN6, and MN10^a

no. of SDSN molecules	SDS		SDSN	
	tot. $\langle S_{CD} \rangle$	gauche defects	tot. $\langle S_{CD} \rangle$	gauche defects
2	0.123	2.8	0.236	2.9
6	0.130	2.6	0.215	2.0
10	0.167	2.7	0.169	2.5

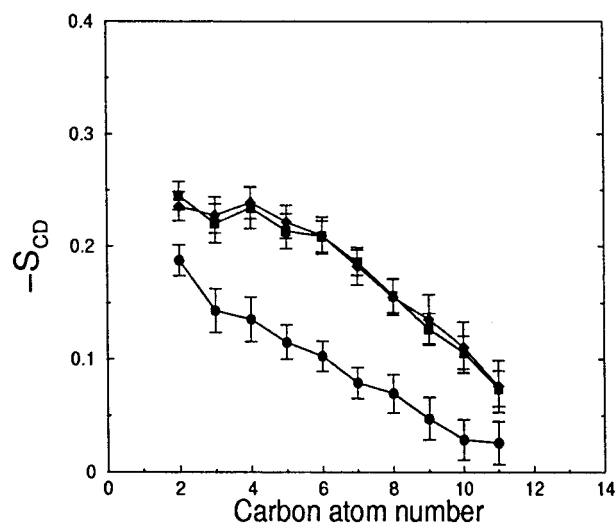
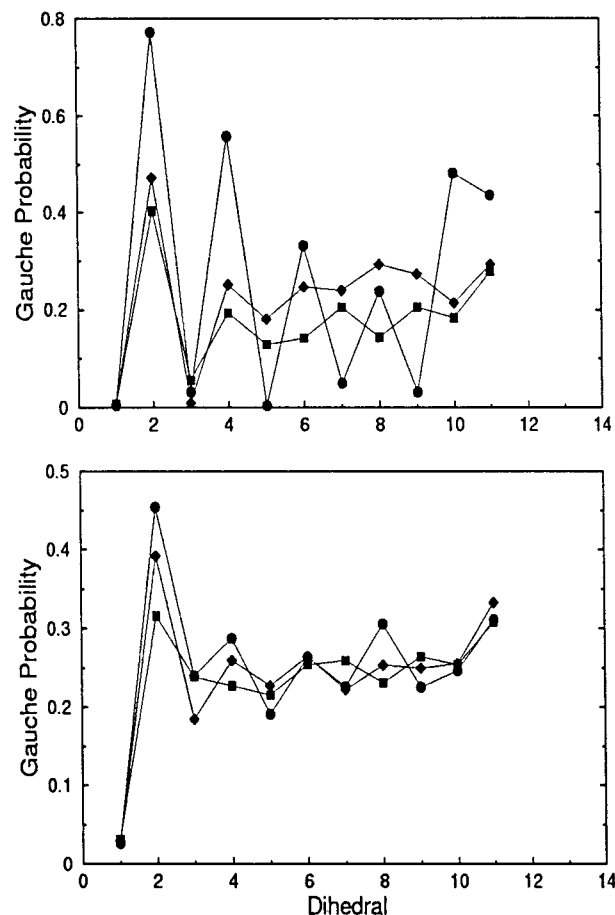
^a The number of SDS molecules is fixed to 38.**TABLE 6: Total Average Order Parameter, $\langle |S_{CD}| \rangle$, and Average Number of Gauche Defects of the SDS Tails in the Single Monolayer, M40, M44, and M48**

no. of SDS molecules	tot. $\langle S_{CD} \rangle$	no. of gauche defects
40	0.093	2.6
44	0.177	2.6
48	0.179	2.5

in the monolayer (bottom picture). The S_{CD} order parameter of the carbons in the SDSN molecules presents different features. The order of carbons 2 and 3 for monolayers MN2, MN6, and MN10 has almost the same value. Nevertheless, the order of the last carbons for the same mixtures gets lower as the SDSN concentration increases. Although it is hard to define any plateau region in any plot of the S_{CD} order parameter in Figure 9, the order of the carbons, as a general trend, decreases down the chain, indicating that the last carbons in the chain are distributed in a more isotropical way. Regardless of the behavior of the S_{CD} order for all the mixtures, it is important to note that as a general feature, the S_{CD} order parameter in the hydrocarbon chains of the SDSN molecules is higher than that in the hydrocarbon chains of the SDS molecules for the same monolayer. Probably a better representation of the order of the tails is given by the quantity $\langle |S_{CD}| \rangle$, which is the average order parameter over all the carbons in the chain. Results of this parameter for the three different monolayer mixtures are given in Table 5. From these data we see that in all cases the average order parameter over all the tails is always higher for the carbons in the SDSN tails than for the carbons of the SDS tails.

To see the effect of the SDSN surfactant over the SDS, we compared the same average $\langle |S_{CD}| \rangle$ order parameter of the single SDS monolayer with that in the monolayer mixture for the same surface coverage. The average order parameter of M40, M44, and M48 is included in Table 6. It can be observed that the average order parameter over the entire tail is higher for the SDS molecules in the single monolayer than that of the SDS in the mixture at the same surface coverage except for M40 in the single monolayer. In Figure 10 we show the S_{CD} order parameter as a function of the carbon atom position for the one component monolayer. Here, the order in the carbons is in general higher as the number of SDS molecules increases. The order in the carbons of the M44 and M48 tails has a similar value.

The ordering of the hydrocarbon tails can also be characterized by the average number of gauche defects. The probabilities of gauche defects in the carbons of SDS and SDSN give us more insight about the conformation of the tails. In Figure 11, the probability of gauche defects for each carbon in the tail is shown. Once more, we have separated the cases of the SDS and SDSN molecules in the mixture. First, we investigated the probability of gauche defects for the SDS carbons (bottom plot of Figure 11). In all the monolayers the first dihedral (S—O—C₁—C₂) is always almost trans. The second dihedral is approximately 55–60% trans for MN2 and MN10, and for MN6 this value is higher, approximately 70% trans. The gauche

**Figure 10.** S_{CD} order parameter as a function of the carbon position of the SDS one component monolayer. Circles are for M40, squares are for M44, and diamonds represent M48.**Figure 11.** Probability of gauche defects as a function of carbon position of the surfactant molecules in the SDS/SDSN monolayer mixture. The top picture is the gauche probability in the SDSN tails, and the bottom picture is the gauche probability in the SDS tails in the same monolayer for all the mixtures. Circles are for MN2, squares are for MN6, and diamonds correspond to MN10.

probability for the rest of the carbons oscillates with a tendency of decreasing trans conformation of the last carbons. The probability of gauche defects in SDSN tails are shown on the top of Figure 11. Interesting is the case of MN2 where the first dihedral (S—O—C₁—C₂) is nearly all trans while the following dihedral has only 20% trans character. The next dihedrals present

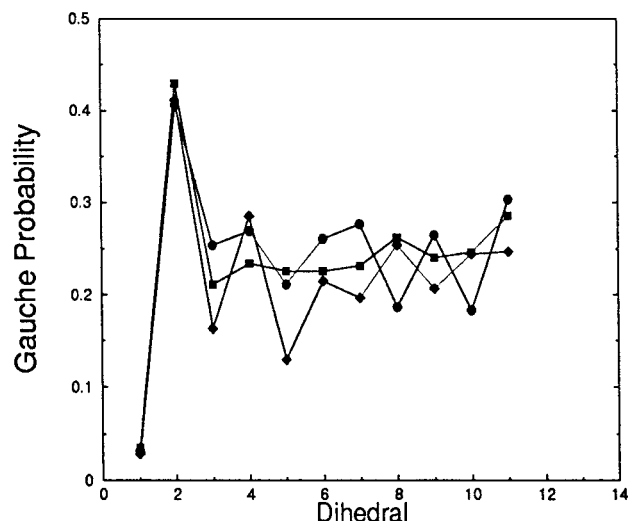


Figure 12. Probability of gauche defects as a function of carbon position in the SDS one component monolayer. Circles are for M40, squares are for M44, and diamonds correspond to M48.

a zigzag shape from high to low probability of gauche defects. Monolayer MN6 has also a high trans conformation in the first carbon (the trans conformation is even higher than that observed for the first carbon in SDS) and 60% trans in the next second carbon. Dihedral 3 of the SDSN molecules has a low probability of gauche defect compare with the same dihedral of the SDS, indicating that it is nearly trans. In Table 5, the average number of gauche defects of the SDS and SDSN tails in each monolayer mixture is given. As a general feature we observe that the SDS tails have, on average, a higher probability of gauche defects than the SDSN tails. To make a comparison of the SDS molecules in the mixture and in the one component monolayer, we calculated the probability of gauche defects of the carbons of the SDS tails in the single monolayer (see Figure 12). From Figures 11 and 12 we observe that the mixture and the single monolayer the S—O—C₁—C₂ dihedral has almost the same value. We also note in Figure 12 that the probability of gauche defects of the second dihedral is almost the same for all the single monolayers. This feature differs from the mixture, where the probability of gauche defects in the second dihedral of the SDS tails depends on the mixture concentration (see bottom of Figure 11). The average number of gauche defects in the SDS tails of the single monolayers is given in Table 6. From this table we found that the average number of gauche defects of the SDS tails in the mixture is equal to or slightly higher than that in the SDS tails in the single monolayer.

4. Conclusions and Discussion

We performed a series of molecular dynamics computer simulations on a SDS/nonionic mixture at the water/CCl₄ interface. We used two different nonionic molecules (SDSN and SDSE) that were prepared with the same SDS molecular structure but with a different charge distribution to have a zero total net charge. We studied the structural properties of the anionic and nonionic surfactants in the monolayer. The headgroup profiles of the SDS and nonionic molecules in the monolayer mixture indicate that they are displaced. From our results we saw how the charge distribution of the molecules affects the position of the surfactants in the interface. In the SDS/SDSN system, the SDS headgroups are slightly shifted to the right of the SDSN. This effect seem to be in the opposite direction, as found in experiments of SDS/dodecanol at the air/water interface.²³ However, if we simulate the monolayer

mixture SDS/SDSE, the locations of the surfactants are in the same direction as indicated by the experiments; i.e., the anionic molecule is shifted more into the water than the nonionic molecule. We recall that the difference between the two nonionic molecules is the charge distribution in their headgroups, mainly the negative charge sites were replaced by positives and vice versa. Even though both nonionic molecules (SDSN and SDSE) are neutral, the interaction with the SDS and water molecules (which depends on the charge distribution of the molecules) determines the positions of the surfactants along the interface.

We also measured the difference in the electrostatic potential across the interface and we found that for the MN monolayers this difference increases with the number of SDSN molecules in the mixture. However, for the ME monolayers the reverse trend occurs: the potential difference decreases as the concentration of SDSE increases.

Finally, we also investigated the tail configuration of the SDS/SDSN monolayer mixture. Studies of surfactant mixtures were investigated experimentally by some authors who were interested in the thickness and inclination of molecule chains, among other properties.^{16,19,21–23,26} So, we conducted studies of some of these properties in order to understand better how the structure of the surfactants is influenced by the concentration or interaction of the nonionic with the anionic molecules. Analyzing the thickness of the SDS and the SDSN surfactants in the same monolayer, we found that the SDSN hydrocarbon chains are larger than the SDS chains. The SDSN tails seem to be more straight than those of the SDS in the mixture. When we compare the tail lengths of the SDS molecules in the single monolayer with those in the mixture, we found that the tails have nearly the same extent and they also have similar inclinations with respect to the surface normal.

The order of the tails in the SDSN molecules is always higher than that in the tails of the SDS molecules in the same mixture. At the same time, the probability of gauche defects of the tails in the mixture show that the SDSN tails present in general more trans conformation than the tails of the SDS. Comparison of the average $\langle |S_{CD}| \rangle$ order parameter of the SDS chains in the mixture and in the single monolayer indicate that the chains are slightly more disordered in the mixture (at high SDSN concentration) than in the single monolayer. As a general feature, we see that somehow the interaction SDSN—SDS induces more tilt and more disorder in the SDS tails than the interaction SDS—SDS. There is also an interesting feature for the monolayer mixtures in the conformation of the surfactants. As the concentration of SDSN molecules increases, the tails of these molecules bend more while the tails of the SDS molecules become straighter. At the same time, the SDSN tails become more disordered while the tails of the SDS molecules are more ordered.

As mentioned before, due to the model of the nonionic molecules, the comparison with experiments is not straightforward. However, in some cases it was possible to observe tendencies shown in experiments. Therefore, these simulations would give us more insight about the role of the molecule polar headgroup and the charge distribution in the behavior of a mixture monolayer.

Acknowledgment. Simulations were performed on a SGI Origin 2000 at the National University of Mexico, DGSCA, UNAM. I am also grateful to Dr. M. Rivera for careful reading of the manuscript.

References and Notes

- (1) Piasecki, D. A.; Wirth, M. J. *J. Phys. Chem.* **1993**, *97*, 7700.

- (2) Lu, J. R.; Marrocco, A.; Su, T. J.; Thomas, R. K.; Penfold, J. *J. Colloid Interface Sci.* **1993**, *158*, 303.
- (3) Tian, Y.; Umemura, J.; Takenaka, T. *Langmuir* **1988**, *4*, 1064.
- (4) Higgins, D. A.; Naujok, R. R.; Corn, R. M. *Chem. Phys. Lett.* **1993**, *213*, 485.
- (5) Conboy, J. C.; Messmer, M. C.; Richmond, G. *J. Phys. Chem. B* **1997**, *101*, 6724.
- (6) Conboy, J. C.; Messmer, M. C.; Richmond, G. *J. Phys. Chem.* **1996**, *100*, 7617.
- (7) Conboy, J. C.; Messmer, M. C.; Richmond, G. *Langmuir* **1998**, *14*, 6722.
- (8) Zhang, Z. H.; Tsuyumoto, I.; Kitamori, T.; Sawada, T. *J. Phys. Chem. B* **1998**, *102*, 10284.
- (9) Lyttle, D. J.; Lu, J. R.; Su, T. J.; Thomas, R. K.; Penfold, J. *Langmuir* **1995**, *11*, 1001.
- (10) Lu, J. R.; Hromadova, M.; Simister, E. A.; Thomas, R. K.; Penfold, J. *J. Phys. Chem.* **1994**, *98*, 11519.
- (11) Goloub, T. P.; Pugh, R. J.; Zhumd, B. V. *J. Colloid Interface Sci.* **2000**, *229*, 72.
- (12) Kunieda, H.; Ozawa, K.; Aramaki, K.; Nakano, A.; Solans, C. *Langmuir* **1998**, *14*, 260.
- (13) Dai, L.; Li, W.; Hou, X. *Colloids Surf., A* **1997**, *125*, 27.
- (14) FilipovicVincekovic, N.; Juranovic, I.; Grahek, Z. *Colloids Surf., A* **1997**, *125*, 115.
- (15) McKenna, C. E.; Knock, M. M.; Bain, C. D. *Langmuir* **2000**, *16*, 5853.
- (16) Bumajdad, A.; Eastoe, J.; Griffiths, P.; Steytler, D. C.; Heenan, R. K.; Lu, J. R.; Timmins, P. *Langmuir* **1999**, *15*, 5271.
- (17) Kronberg, B. *Curr. Opin. Colloid Interface Sci.* **1997**, *2*, 456.
- (18) Rosen, M. J.; Hua, X. Y. *J. Colloid Interface Sci.* **1982**, *86*, 164.
- (19) Penfold, J.; Staples, E. J.; Tucker, I.; Thomas, R. K. *Colloids Surf., A* **1999**, *155*, 11.
- (20) Penfold, J.; Staples, E.; Tucker, I.; Soubiran, L.; Creeth, A.; Hubbard, J. *Phys. Chem. Chem. Phys.* **2000**, *2*, 5230.
- (21) Penfold, J.; Staples, E.; Tucker, I.; Thomas, R. K. *J. Colloid Interface Sci.* **1998**, *201*, 223.
- (22) Penfold, J.; Staples, E.; Tucker, I.; Soubiran, L.; Lodi, A. K.; Thompson, L.; Thomas, R. K. *Langmuir* **1998**, *14*, 2139.
- (23) Lu, J. R.; Purcell, I. P.; Lee, E. M.; Simister, E. A.; Thomas, R. K.; Rennie, A. R.; Penfold, J. *J. Colloid Interface Sci.* **1995**, *174*, 441.
- (24) Holland, P. M. *Colloids Surf., A* **1986**, *19*, 171.
- (25) Nikas, Y. F.; Pruvada, S.; Blankschtein, D. *Langmuir* **1997**, *8*, 22680.
- (26) Shiloach, A.; Blankschtein, D. *Langmuir* **1998**, *14*, 7166.
- (27) Mulqueen, M.; Blankschtein, D. *Langmuir* **2000**, *16*, 7640.
- (28) Mulqueen, M.; Blankschtein, D. *Langmuir* **2002**, *18*, 365.
- (29) Mulqueen, M.; Blankschtein, D. *Langmuir* **1999**, *15*, 8832.
- (30) Fainerman, V. B.; Vollhardt, D.; Emrich, G. *J. Phys. Chem. B* **2001**, *105*, 4324.
- (31) Kuhn, H.; Rehage, H. *J. Phys. Chem. B* **1999**, *103*, 8493.
- (32) Schweighofer, K. J.; Essmann, U.; Berkowitz, M. *J. Phys. Chem. B* **1997**, *101*, 3793.
- (33) Schweighofer, K. J.; Essmann, U.; Berkowitz, M. *J. Phys. Chem. B* **1997**, *101*, 10775.
- (34) Michel, D.; Benjamin, I. *J. Phys. Chem. B* **1998**, *102*, 5145.
- (35) Okamura, E.; Fukushima, N.; Hayashi, S. *Langmuir* **1999**, *15*, 3589.
- (36) Dominguez, H.; Berkowitz, M. L. *J. Phys. Chem. B* **2000**, *104*, 5302.
- (37) Forester, T. R.; Smith, W. DL-POLY Package of Molecular Simulation; CCLRC, Daresbury Laboratory: Daresbury, Warrington, England 1996.
- (38) Hoover, W. G. *Phys. Rev. A* **1985**, *31*, 1695.
- (39) In-Chul, Y.; Berkowitz, M. L. *J. Chem. Phys.* **1999**, *111*, 3155.
- (40) Grubb, S. G.; Kim, M. W.; Rasing, Th.; Shen, Y. R. *Langmuir* **1988**, *4*, 452.
- (41) Tsujii, K. In *Surface Activity, Principles, Phenomena and Applications*; Academic Press: New York 1998; p 4.
- (42) Egberts, E.; Berendsen, H. J. C. *J. Chem. Phys.* **1988**, *89*, 3718.